

Bayesian co-estimation of selfing rate and locus-specific mutation rates for a partially selfing population

Benjamin D. Redelings, Seiji Kumagai, Andrei Tatarenkov, Ann K. Sakai, Stephen G. Weller, John C. Avise, and Marcy K. Uyenoyama

Abstract

We present a Bayesian method for characterizing the mating system of populations reproducing through a mixture of self-fertilization and random outcrossing. Our method uses patterns of genetic variation across the genome as a basis for inference about pure hermaphroditism, androdioecy, and gynodioecy. We extend the standard coalescence model to accommodate these mating systems, accounting explicitly for multilocus identity disequilibrium, inbreeding depression, and variation in fertility among mating types. We incorporate the Ewens Sampling Formula (ESF) under the infinite-alleles model of mutation to obtain a novel expression for the likelihood of mating system parameters. Our Markov chain Monte Carlo (MCMC) algorithm assigns locus-specific mutation rates, drawn from a common mutation rate distribution that is itself estimated from the data using a Dirichlet Process Prior (DPP) model. Among the parameters jointly inferred are the population-wide rate of self-fertilization, locus-specific mutation rates, and the number of generations since the most recent outcrossing event for each sampled individual.

1 Introduction

Inbreeding has pervasive consequences throughout the genome, affecting population-level relationships between genes at each locus and among loci. This generation of genome-wide, multilocus disequilibria of various orders transforms the context in which evolution proceeds. Here, we address a simple form of inbreeding: a mixture of self-fertilization (selfing) and random outcrossing (Clegg, 1980; Ritland, 2002).

A variety of methods exist for the estimation of selfing rates from genetic data. Wright's (1921) fundamental approach bases the estimation of selfing rates on the coefficient of inbreeding (F_{IS}), which reflects the departure from Hardy-Weinberg proportions of genotypes for a given set of allele frequencies. The maximum likelihood method of Enjalbert and David (2000) detects inbreeding from departures of multiple loci from Hardy-Weinberg proportions, accounting for correlations in heterozygosity among loci (identity disequilibrium, Cockerham and Weir, 1968) and estimating allele frequencies for each locus. David et al. (2007) extend the approach of Enjalbert and David (2000), basing the estimation of selfing rates on the

distribution of heterozygotes across multiple, unlinked loci, while accommodating errors in scoring heterozygotes as homozygotes. A primary objective of **InStruct** (Gao et al., 2007) is the estimation of admixture. It extends the widely-used program **structure** (Pritchard et al., 2000), which bases the estimation of admixture on disequilibria of various forms, by accounting for disequilibria due to selfing. Progeny array methods (see Ritland, 2002), which base the estimation of selfing rates on the genetic analysis of progeny for which one or more parents are known, are particularly well-suited to plant populations. Wang et al. (2012) extend this approach to a random sample of individuals by reconstructing sibship relationships within the sample.

Methods that base the estimation of inbreeding rates on the observed departure from random union of gametes require information on expected Hardy-Weinberg proportions. Population-wide frequencies of alleles observed in a sample at locus l ($\{p_{li}\}$) can be estimated jointly in a maximum-likelihood framework (*e.g.*, Hill et al., 1995) or integrated out as nuisance parameters in a Bayesian framework (*e.g.*, Ayres and Balding, 1998). Similarly, locus-specific heterozygosity

$$d_l = 1 - \sum_i p_{li}^2 \quad (1)$$

can be obtained from observed allele frequencies (Enjalbert and David, 2000) or estimated directly and jointly with the selfing rate (David et al., 2007).

In contrast, our Bayesian method for the analysis of partial self-fertilization derives from a coalescence model that accounts for genetic variation and uses the Ewens Sampling Formula (ESF, Ewens, 1972). Our approach replaces the estimation of allele frequencies or heterozygosity (1) by the estimation of a locus-specific mutation rate (θ^*) under the infinite-alleles model of mutation. We use a Dirichlet Process Prior (DPP) to determine the number of classes of mutation rates, the mutation rate for each class, and the class membership of each locus. We assign the DPP parameters in a conservative manner so that it creates a new mutational class only if sufficient evidence exists to justify doing so. Further, while other methods assume that the frequency in the population of an allelic class not observed in the sample is zero, the ESF provides the probability, under the infinite-alleles model of mutation, that the next-sampled gene represents a novel allele (see (21)).

To estimate the probability that a random individual is uniparental (s^*), we exploit identity disequilibrium (Cockerham and Weir, 1968), the correlation in heterozygosity across loci. This association, even among unlinked loci, reflects that all loci within an individual share a history of inbreeding back to the most recent random outcrossing event. Conditional on the number of generations since this event, the genealogical histories of unlinked loci are independent. Our method infers the number of consecutive generations of self-fertilization in the immediate ancestry of each sampled diploid individual and the probability of coalescence during this period between the lineages at each locus.

In inferring the full likelihood from the observed frequency spectrum of diploid genotypes at multiple unlinked loci, we determine the distributions of the allele frequency spectra ancestral to the sample at the most recent point at which all sampled gene lineages at each locus reside in separate individuals. At this point, the ESF provides the exact likelihood, obviating the need for further genealogical reconstruction. This approach permits computationally efficient analysis of large samples of individuals with large numbers of observed loci

across the genome.

Here, we address the estimation of inbreeding rates in populations undergoing pure hermaphroditism, androdioecy (hermaphrodites and males), or gynodioecy (hermaphrodites and females). Our method provides a means for the simultaneous inference of various aspects of the mating system, including the population proportions of sexual forms and levels of inbreeding depression. We apply our method to simulated data sets to demonstrate its level of accuracy and to show that it provides accurate assessments of uncertainty. We also apply it to microsatellite data from the androdioecious killifish *Kryptolebias marmoratus* (Mackiewicz et al., 2006; Tatarenkov et al., 2012) and to the gynodioecious Hawaiian endemic *Schiedea salicaria* (Wallace et al., 2011).

2 Evolutionary model

2.1 Rates of coalescence and mutation

In large populations, switching of lineages between uniparental and biparental carriers occurs on the order of generations, virtually instantaneously relative to the rate at which lineages residing in distinct individuals coalesce (Nordborg and Donnelly, 1997; Fu, 1997). Here, we describe the structure of the coalescence process shared by our models of pure hermaphroditism, androdioecy, and gynodioecy.

Uniparental proportion and the rate of parent-sharing: In populations reproducing through a mixture of self-fertilization and random outcrossing, the rate of coalescence is determined by the probability that a random individual is uniparental (s^* , the uniparental proportion) and the rate at which genetic lineages sampled from distinct individuals derive from the same individual in the immediately preceding generation ($1/N^*$, the rate of parent-sharing).

For a given breeding system, s^* denotes the probability that a random individual is uniparental. Under pure hermaphroditism, for example, s^* corresponds to

$$s_H = \frac{\tilde{s}\tau}{\tilde{s}\tau + 1 - \tilde{s}}, \quad (2a)$$

for \tilde{s} the fraction of uniparental offspring at conception and τ the rate of survival of uniparental relative to biparental offspring. Also under pure hermaphroditism, the probability that a pair of genes, randomly sampled from distinct individuals, derive from the same individual in the immediately preceding generation is

$$1/N_H = [s_H^2 + 4s_H(1 - s_H)(1/2) + 4(1 - s_H)^2(1/4)] / N_h = 1/N_h, \quad (2b)$$

independent of the rates of inbreeding and inbreeding depression (see Appendix A).

These expressions (2), which assume pure hermaphroditism, are equivalent to those obtained by Fu (1997) and Nordborg and Donnelly (1997). In androdioecious populations, comprising N_h reproducing hermaphrodites and N_m reproducing males (female-steriles), the uniparental proportion (s^*) is identical to the case of pure hermaphroditism (2a)

$$s_A = \frac{\tilde{s}\tau}{\tilde{s}\tau + 1 - \tilde{s}}, \quad (3a)$$

and a pair of genes sampled from distinct individuals derive from the same parent ($1/N^*$) with probability

$$\frac{1}{N_A} = \frac{(1 + s_A)^2}{4N_h} + \frac{(1 - s_A)^2}{4N_m}. \quad (3b)$$

In the absence of inbreeding ($s_A = 0$), this expression reduces to the classical harmonic mean expression for effective population size (Wright, 1969). In gynodioecious populations, comprising N_h reproducing hermaphrodites and N_f reproducing females (male-steriles), the uniparental proportion (s^*) corresponds to

$$s_G = \frac{\tau N_h a}{\tau N_h a + N_h(1 - a) + N_f \sigma}, \quad (4a)$$

in which σ represents the seed fertility of females relative to hermaphrodites and a the proportion of seeds of hermaphrodites set by self-pollen. The probability that a pair of genes sampled from distinct individuals derive from the same parent ($1/N^*$) is

$$\frac{1}{N_G} = \frac{[2 - (1 - s_G)(1 - H)]^2}{4N_h} + \frac{[(1 - s_G)(1 - H)]^2}{4N_f}, \quad (4b)$$

in which

$$H = \frac{N_h(1 - a)}{N_h(1 - a) + N_f \sigma} \quad (5)$$

represents the proportion of biparental offspring that have a hermaphroditic seed parent. Appendix A presents full derivations of the uniparental proportion s^* and the rate of parent-sharing $1/N^*$ under the three reproductive systems considered here.

Relative rates of coalescence and mutation: Fundamental to coalescence-based analyses of patterns of genetic variation is the rate of coalescence of genetic lineages, which depends on the uniparental fraction (s^*) and the rate of parent-sharing ($1/N^*$), relative to the rate of mutation.

We have determined for three iconic mating systems the rate of parent-sharing $1/N^*$, the probability that a pair of genes sampled from distinct individuals derive from the same individual in the immediately preceding generation. The two lineages descend from the same gene (immediate coalescence) or from distinct genes in that individual with equal probability. In the latter case, the individual is either uniparental (probability s^*), implying descent once again of the lineages from a single individual in the preceding generation, or biparental, implying descent from distinct parents. Residence of a pair of lineages in a single individual rapidly resolves either to coalescence, with probability

$$f_c = \frac{s^*}{2 - s^*}, \quad (6)$$

or to residence in distinct individuals, with the complement probability. This expression is identical to the classical coefficient of identity (Wright, 1921; Haldane, 1924). The total rate of coalescence of lineages sampled from distinct individuals corresponds to

$$\frac{(1 + f_c)/2}{N^*} = \frac{1}{N^*(2 - s^*)}. \quad (7)$$

Let u denote the rate of mutation under the infinite alleles model and $1/N^*$ the rate at which a pair of lineages in distinct individuals derive in the immediately preceding generation from the same individual (parent-sharing). Our model assumes that parent-sharing and mutation occur on comparable time scales:

$$\begin{aligned} \lim_{\substack{N \rightarrow \infty \\ u \rightarrow 0}} 4Nu &= \theta \\ \lim_{\substack{N \rightarrow \infty \\ N^* \rightarrow \infty}} N/N^* &= C, \end{aligned} \tag{8}$$

for θ the scaled rate of mutation, C the scaled rate of coalescence, and N an arbitrary quantity that goes to infinity at a rate comparable to N^* and $1/u$ (see Appendix A). Here, C represents the inverse of the effective population size relative to unity for a panmictic monoecious population. For example, C greater than unity implies a higher rate of coalescence (smaller effective population size) than for a monoecious population.

Our model assumes independence between the processes of coalescence and mutation and that these processes occur on a much longer time scale than reproduction:

$$1 - s^* \gg u, 1/N^*. \tag{9}$$

For m lineages, each residing in a distinct individual, the probability that the most recent event corresponds to mutation is

$$\lim_{N \rightarrow \infty} \frac{mu}{mu + \binom{m}{2}/[N^*(2 - s^*)]} = \frac{\theta^*}{\theta^* + m - 1},$$

in which

$$\begin{aligned} \theta^* &= \lim_{\substack{N \rightarrow \infty \\ u \rightarrow 0}} 2N^*u(2 - s^*) = \lim_{\substack{N \rightarrow \infty \\ u \rightarrow 0}} 4Nu \frac{N^*}{N} (1 - s^*/2) \\ &= \theta(1 - s^*/2)/C, \end{aligned} \tag{10}$$

for θ and C defined in (8). This key expression for θ^* determines the probability of the observed pattern of variation under the infinite-alleles model of mutation.

2.2 Likelihood

Here, we describe our use of the Ewens Sampling Formula (ESF, Ewens, 1972) to determine likelihoods based on a sample of diploid multilocus genotypes.

Genealogical histories: For a sample comprising up to 2 alleles at each of L autosomal loci in n diploid individuals, we represent the observed genotypes by

$$\mathbf{X} = \{\mathbf{X}_1, \mathbf{X}_2, \dots, \mathbf{X}_L\}, \tag{11}$$

in which \mathbf{X}_l denotes the set of genotypes observed at locus l ,

$$\mathbf{X}_l = \{\mathbf{X}_{l1}, \mathbf{X}_{l2}, \dots, \mathbf{X}_{ln}\}, \tag{12}$$

with

$$\mathbf{X}_{lk} = (X_{lk1}, X_{lk2})$$

the genotype at locus l of individual k , with alleles X_{lk1} and X_{lk2} .

To facilitate accounting for the shared recent history of genes borne by an individual in sample, we introduce latent variables

$$\mathbf{T} = \{T_1, T_2, \dots, T_n\}, \quad (13)$$

for T_k denoting the number of consecutive generations of selfing in the immediate ancestry of the k^{th} individual, and

$$\mathbf{I} = \{I_{lk}\}, \quad (14)$$

for I_{lk} indicating whether the lineages borne by the k^{th} individual at locus l coalesce within the most recent T_k generations. Independent of other individuals, the number of consecutive generations of inbreeding in the ancestry of the k^{th} individual is geometrically distributed:

$$T_k \sim \text{Geometric}(s^*), \quad (15)$$

with $T_k = 0$ signifying that individual k is the product of random outcrossing. Irrespective of whether 0, 1, or 2 of the genes at locus l in individual k are observed, I_{lk} indicates whether the two genes at that locus in individual k coalesce during the T_k consecutive generations of inbreeding in its immediate ancestry:

$$I_{lk} = \begin{cases} 0 & \text{if the two genes do not coalesce} \\ 1 & \text{if the two genes coalesce.} \end{cases}$$

Because the pair of lineages at any locus coalesce with probability $\frac{1}{2}$ in each generation of selfing,

$$\Pr(I_{lk} = 0) = \frac{1}{2^{T_k}} = 1 - \Pr(I_{lk} = 1). \quad (16)$$

Figure 1 depicts the recent genealogical history at a locus l in 5 individuals. Individuals 2 and 5 are products of random outcrossing ($T_2 = T_5 = 0$), while the others derive from some positive number of consecutive generations of selfing in their immediate ancestry ($T_1 = 2, T_3 = 3, T_4 = 1$). Both individuals 1 and 3 are homozygotes ($\alpha\alpha$), with the lineages of individual 3 but not 1 coalescing more recently than the most recent outcrossing event ($I_{l1} = 0, I_{l3} = 1$). As individual 2 is heterozygous ($\alpha\beta$), its lineages necessarily remain distinct since the most recent outcrossing event ($I_{l2} = 0$). One gene in each of individuals 4 and 5 are unobserved (*), with the unobserved lineage in individual 4 but not 5 coalescing more recently than the most recent outcrossing event ($I_{l4} = 1, I_{l5} = 0$).

In addition to the observed sample of diploid individuals, we consider the state of the sampled lineages at the most recent generation in which an outcrossing event has occurred in the ancestry of all n individuals. This point in the history of the sample occurs \hat{T} generations into the past, for

$$\hat{T} = 1 + \max_k T_k.$$

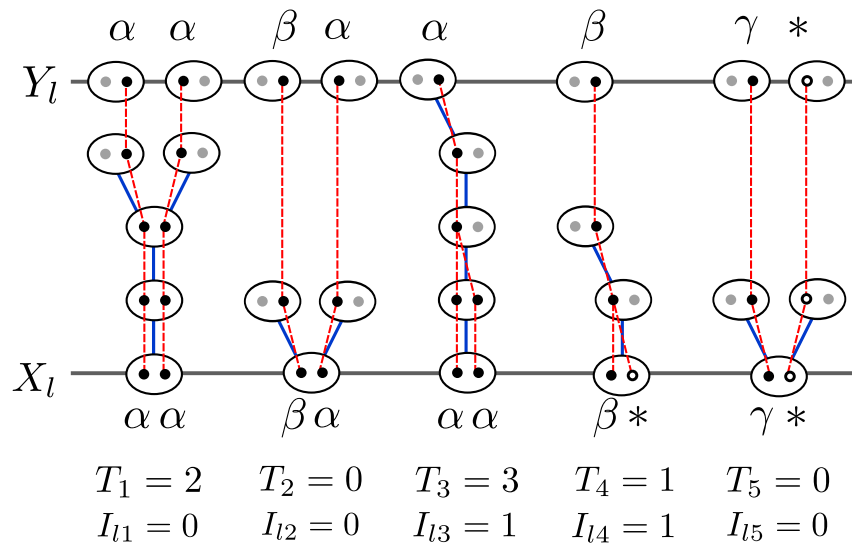


Fig. 1: Following the history of the sample (\mathbf{X}_l) backwards in time until all ancestors of sampled genes reside in different individuals (\mathbf{Y}_l). Ovals represent individuals and dots represent genes. Blue lines indicate the parents of individuals, while red lines represent the ancestry of genes. Filled dots represent sampled genes for which the allelic class is observed (Greek letters) and their ancestral lineages. Open dots represent genes in the sample with unobserved allelic class (*). Grey dots represent other genes carried by ancestors of the sampled individuals. The relationship between the observed sample \mathbf{X}_l and the ancestral sample \mathbf{Y}_l is determined by the intervening coalescence events \mathbf{I}_l . \mathbf{T} indicates the number of consecutive generations of selfing for each sampled individual.

In Fig. 1, for example, $\hat{T} = 4$, reflecting the most recent outcrossing event in the ancestry of individual 3. The ESF provides the probability of the allele frequency spectrum at this point.

We represent the ordered list of allelic states of the lineages at \hat{T} generations into the past by

$$\mathbf{Y} = \{\mathbf{Y}_1, \mathbf{Y}_2, \dots, \mathbf{Y}_L\}, \quad (17)$$

for \mathbf{Y}_l a list of ancestral genes in the same order as their descendants in \mathbf{X}_l . Each gene in \mathbf{Y}_l is the ancestor of either 1 or 2 genes at locus l from a particular individual in \mathbf{X}_l (12), depending on whether the lineages held by that individual coalesce during the consecutive generations of inbreeding in its immediate ancestry. We represent the number of genes in \mathbf{Y}_l by m_l ($n \leq m_l \leq 2n$). In Figure 1, for example, \mathbf{X}_l contains 10 genes in 5 individuals, but \mathbf{Y}_l contains only 8 genes, with Y_{l1} the ancestor of only the first allele of \mathbf{X}_{l1} and Y_{l5} the ancestor of both alleles of \mathbf{X}_{l3} .

We assume (9) that the initial phase of consecutive generations of selfing is sufficiently short to ensure a negligible probability of mutation in any lineage at any locus and a negligible probability of coalescence between lineages held by distinct individuals more recently than \hat{T} . Accordingly, the coalescence history \mathbf{I} (14) completely determines the correspondence between genetic lineages in \mathbf{X} (11) and \mathbf{Y} (17).

Computing the likelihood: In principle, the likelihood of the observed data can be computed from the augmented likelihood by summation:

$$\Pr(\mathbf{X}|\Theta^*, s^*) = \sum_{\mathbf{I}} \sum_{\mathbf{T}} \Pr(\mathbf{X}, \mathbf{I}, \mathbf{T}|\Theta^*, s^*), \quad (18)$$

for

$$\Theta^* = \{\theta_1^*, \theta_2^*, \dots, \theta_L^*\} \quad (19)$$

the list of scaled, locus-specific mutation rates, s^* the population-wide uniparental proportion for the reproductive system under consideration (*e.g.*, (2a) for the pure hermaphroditism model), and \mathbf{T} (13) and \mathbf{I} (14) the lists of latent variables representing the time since the most recent outcrossing event and whether the 2 lineages borne by a sampled individual coalesce during this period. Here we follow a common abuse of notation in using $\Pr(\mathbf{X})$ to denote $\Pr(\mathbf{X} = \mathbf{x})$ for random variable \mathbf{X} and realized value \mathbf{x} . Summation (18) is computationally expensive: the number of consecutive generations of inbreeding in the immediate ancestry of an individual (T_k) has no upper limit (compare David et al., 2007) and the number of combinations of coalescence states (I_{lk}) across the L loci and n individuals increases exponentially (2^{Ln}) with the total number of assignments. We perform Markov chain Monte Carlo (MCMC) to avoid both these sums.

To calculate the augmented likelihood, we begin by applying Bayes rule:

$$\Pr(\mathbf{X}, \mathbf{I}, \mathbf{T}|\Theta^*, s^*) = \Pr(\mathbf{X}, \mathbf{I}|\mathbf{T}, \Theta^*, s^*) \Pr(\mathbf{T}|\Theta^*, s^*).$$

Because the times since the most recent outcrossing event \mathbf{T} depend only on the uniparental proportion s^* , through (15), and not on the rates of mutation Θ^* ,

$$\Pr(\mathbf{T}|\Theta^*, s^*) = \prod_{k=1}^n \Pr(T_k|s^*).$$

Even though our model assumes the absence of physical linkage among any of the loci, the genetic data \mathbf{X} and coalescence events \mathbf{I} are not independent across loci because they depend on the times since the most recent outcrossing event \mathbf{T} . Given \mathbf{T} , however, the genetic data and coalescence events are independent across loci

$$\Pr(\mathbf{X}, \mathbf{I} | \mathbf{T}, \Theta^*, s^*) = \prod_{l=1}^L \Pr(\mathbf{X}_l, \mathbf{I}_l | \mathbf{T}, \theta_l^*, s^*).$$

Further,

$$\begin{aligned} \Pr(\mathbf{X}_l, \mathbf{I}_l | \mathbf{T}, \theta_l^*, s^*) &= \Pr(\mathbf{X}_l | \mathbf{I}_l, \mathbf{T}, \theta_l^*, s^*) \cdot \Pr(\mathbf{I}_l | \mathbf{T}, \theta_l^*, s^*) \\ &= \Pr(\mathbf{X}_l | \mathbf{I}_l, \theta_l^*, s^*) \cdot \prod_{k=1}^n \Pr(I_{lk} | T_k). \end{aligned}$$

This expression reflects the fact that the times to the most recent outcrossing event \mathbf{T} affect the observed genotypes \mathbf{X}_l only through the coalescence states \mathbf{I}_l and that the coalescence states \mathbf{I}_l depend only on the times to the most recent outcrossing event \mathbf{T} , through (16).

To compute $\Pr(\mathbf{X}_l | \mathbf{I}_l, \theta_l^*, s^*)$, we incorporate latent variable \mathbf{Y}_l (17), describing the states of lineages at the most recent point at which all occur in distinct individuals (Fig. 1):

$$\begin{aligned} \Pr(\mathbf{X}_l | \mathbf{I}_l, \theta_l^*, s^*) &= \sum_{\mathbf{Y}_l} \Pr(\mathbf{X}_l, \mathbf{Y}_l | \mathbf{I}_l, \theta_l^*, s^*) \\ &= \sum_{\mathbf{Y}_l} \Pr(\mathbf{X}_l | \mathbf{Y}_l, \mathbf{I}_l, \theta_l^*, s^*) \Pr(\mathbf{Y}_l | \mathbf{I}_l, \theta_l^*, s^*) \\ &= \sum_{\mathbf{Y}_l} \Pr(\mathbf{X}_l | \mathbf{Y}_l, \mathbf{I}_l) \cdot \Pr(\mathbf{Y}_l | \mathbf{I}_l, \theta_l^*), \end{aligned} \quad (20a)$$

reflecting that the coalescence states \mathbf{I}_l establish the correspondence between the spectrum of genotypes in \mathbf{X}_l and the spectrum of alleles in \mathbf{Y}_l and that the distribution of \mathbf{Y}_l , given by the ESF, depends on the uniparental proportion s^* only through the scaled mutation rate θ_l^* (10).

Given the sampled genotypes \mathbf{X}_l and coalescence states \mathbf{I}_l , at most one ordered list of alleles \mathbf{Y}_l produces positive $\Pr(\mathbf{X}_l | \mathbf{Y}_l, \mathbf{I}_l)$ in (20a). Coalescence of the lineages at locus l in any heterozygous individual (*e.g.*, $X_{lk} = (\beta, \alpha)$ with $I_{lk} = 1$ in Fig. 1) implies

$$\Pr(\mathbf{X}_l | \mathbf{Y}_l, \mathbf{I}_l) = 0$$

for all \mathbf{Y}_l . Any non-zero $\Pr(\mathbf{X}_l | \mathbf{Y}_l, \mathbf{I}_l)$ precludes coalescence in any heterozygous individual and \mathbf{Y}_l must specify the observed alleles of \mathbf{X}_l in the order of observation, with either 1 ($I_{lk} = 1$) or 2 ($I_{lk} = 0$) instances of the allele for any homozygous individual (*e.g.*, $X_{lk} = (\alpha, \alpha)$). For all cases with non-zero $\Pr(\mathbf{X}_l | \mathbf{Y}_l, \mathbf{I}_l)$,

$$\Pr(\mathbf{X}_l | \mathbf{Y}_l, \mathbf{I}_l) = 1.$$

Accordingly, expression (20a) reduces to

$$\Pr(\mathbf{X}_l | \mathbf{I}_l, \theta_l^*, s^*) = \sum_{\mathbf{Y}_l: \Pr(\mathbf{X}_l | \mathbf{Y}_l, \mathbf{I}_l) \neq 0} \Pr(\mathbf{Y}_l | \mathbf{I}_l, \theta_l^*), \quad (20b)$$

a sum with either 0 or 1 terms. Because all genes in \mathbf{Y}_l reside in distinct individuals, we obtain $\Pr(\mathbf{Y}_l|\mathbf{I}_l, \theta_l^*)$ from the Ewens Sampling Formula for a sample, of size

$$m_l = 2n - \sum_{k=1}^n I_{lk},$$

ordered in the sequence in which the genes are observed.

A well-known property of the ESF (Ewens, 1972; Karlin and McGregor, 1972) is that given the spectrum of alleles observed among $i - 1$ genes, the probability that the next-sampled (i^{th}) gene represents a novel allele corresponds to

$$\pi_i = \frac{\theta^*}{i - 1 + \theta^*}, \quad (21)$$

for θ^* defined in (10), and the probability that it represents an additional copy of allele j is

$$(1 - \pi_i) \frac{i_j}{i - 1},$$

for i_j the number of replicates of allele j already observed ($\sum_j i_j = i - 1$). These expressions provide $\Pr(\mathbf{Y}_l|\mathbf{I}_l, \theta_l^*)$ in (20b). Explicitly, for \mathbf{Y}_l the ordered list of alleles observed in the sample at locus l ,

$$\Pr(\mathbf{Y}_l|\mathbf{I}_l, \theta_l^*) = \frac{(\theta_l^*)^{K_l} \prod_{j=1}^{K_l} (m_{lj} - 1)!}{\prod_{i=1}^{m_l} (i - 1 + \theta_l^*)}, \quad (22)$$

in which K_l denotes the total number of distinct allelic classes, m_{lj} the number of replicates of the j^{th} allele in the sample, and $m_l = \sum_j m_{lj}$ the number of lineages remaining at time \hat{T} (Fig. 1).

Missing data: Our method allows the allelic class of one or both genes at each locus to be missing. In Fig. 1, for example, the genotype of individual 4 is $\mathbf{X}_{l4} = (\beta, *)$, indicating that the allelic class of the first gene is observed to be β , but that of the second gene is unknown.

A missing allelic specification in the sample of genotypes \mathbf{X}_l leads to a missing specification for the corresponding gene in \mathbf{Y}_l unless the genetic lineage coalesces with the lineage of an observed allele in the period between \mathbf{X}_l and \mathbf{Y}_l . Figure 1 illustrates such a coalescence event in the case of individual 4. In contrast, the lineages ancestral to the genes carried by individual 5 fail to coalesce more recently than their separation into distinct individuals, giving rise to a missing specification in \mathbf{Y}_l .

The probability of \mathbf{Y}_l can be computed by simply summing over all possible values for each missing specification. Equivalently, those elements may simply be dropped from \mathbf{Y}_l before computing the probability via the ESF, the procedure implemented in our method.

3 Bayesian inference framework

Derivations presented in the preceding section indicate that the probability of a sample of diploid genotypes under the infinite alleles model depends on only the uniparental proportion

s^* and the scaled mutation rates Θ^* (19) across loci. These parameters are composite parameters that are functions of the basic demographic parameters characterizing each model of reproduction under consideration (Appendix A). As a consequence, the genotypic data provide equal support to any combination of basic parameters that implies the same values of s^* and Θ^* .

Although some basic parameters of a given model may be unidentifiable from the genotypic data alone, our MCMC implementation updates the basic parameters directly, with likelihoods determined from the implied values of s^* and Θ^* . This feature facilitates the incorporation of information in addition to the genotypic data that can contribute to the estimation of the basic parameters under a particular model or assessment of alternative models.

3.1 Prior on mutation rates

Ewens (1972) showed for the panmictic case that the number of distinct allelic classes observed at a locus (*e.g.*, K_l in (22)) provides a sufficient statistic for the estimation of the scaled mutation rate. Because each locus l provides relatively little information about the scaled mutation rate θ_l^* (10), we assume that mutation rates across loci cluster in a finite number of groups. However, we do not know *a priori* the group assignment of loci or even the number of distinct rate classes among the observed loci. We make use of the Dirichlet process prior to estimate simultaneously the number of groups, the value of θ^* for each group, and the assignment of loci to groups.

The Dirichlet process comprises a base distribution, which here represents the distribution of the scaled mutation rate θ^* across groups, and a concentration parameter α , which controls the probability that each successive locus forms a new group. We assign 0.1 to α of the Dirichlet process, and place a gamma distribution ($\Gamma(\alpha = 0.25, \beta = 2)$) on the mean scaled mutation rate for each group. As this prior has a high variance relative to the mean (0.5), it is relatively uninformative about θ^* .

3.2 Models of reproduction

Each of the pure hermaphroditism, androdioecy, and gynodioecy models addressed here comprise a set of demographic parameters Ψ (Appendix A), in addition to the scaled mutation rates Θ^* (19) across loci. We have

$$\begin{aligned} \Pr(\mathbf{X}, \Theta^*, \Psi) &= \Pr(\mathbf{X}|\Theta^*, \Psi) \cdot \Pr(\Theta^*) \cdot \Pr(\Psi) \\ &= \Pr(\mathbf{X}|\Theta^*, s^*(\Psi)) \cdot \Pr(\Theta^*) \cdot \Pr(\Psi), \end{aligned}$$

for \mathbf{X} the genotypic data and $s^*(\Psi)$ the uniparental fraction determined by Ψ for the model under consideration. To determine the marginal distribution of θ_l (8) for each locus l , we use (10), incorporating the distributions of $s^*(\Psi)$ and $C(\Psi)$, the scaling factor defined in (8):

$$\theta_l = \theta_l^* \cdot \frac{C}{1 - s^*/2}. \quad (23)$$

Pure hermaphroditism: For this model, $\Psi = \{\tilde{s}, \tau\}$, where \tilde{s} is the proportion of conceptions through selfing, and τ is the relative viability of uniparental offspring. (Appendix A). We propose uniform priors for \tilde{s} and τ :

$$\begin{aligned}\tilde{s} &\sim \text{Uniform}(0, 1) \\ \tau &\sim \text{Uniform}(0, 1).\end{aligned}$$

Androdioecy: For this model, $\Psi = \{\tilde{s}, \tau, p_m\}$, for p_m (A.2) the proportion of males among reproductives. We propose uniform priors for each of these parameters:

$$\begin{aligned}\tilde{s} &\sim \text{Uniform}(0, 1) \\ \tau &\sim \text{Uniform}(0, 1) \\ p_m &\sim \text{Uniform}(0, 1).\end{aligned}$$

Gynodioecy: For this model, $\Psi = \{a, \tau, p_f, \sigma\}$, including a the proportion of conceptions by hermaphrodites through selfing, p_f (A.4) the proportion of females (male-steriles) among reproductives, and σ the fertility of male-steriles relative to hermaphrodites (Appendix A). We propose uniform priors as follows:

$$\begin{aligned}a &\sim \text{Uniform}(0, 1) \\ \tau &\sim \text{Uniform}(0, 1) \\ p_f &\sim \text{Uniform}(0, 1) \\ 1/\sigma &\sim \text{Uniform}(0, 1).\end{aligned}$$

Additional data: When Ψ contains more than one free parameter, the basic parameters that comprise Ψ are not identifiable from the genetic data alone. One approach to this problem is to incorporate additional data to make these parameters identifiable. For example, under the androdioecious model, a count of n_m males among n_{total} zygotes observed may be incorporated into the likelihood

$$\Pr(\mathbf{X}, \mathbf{I}, \mathbf{T}, n_m | s^*, \Theta^*, p_m, n_{total}) = \Pr(\mathbf{X}, \mathbf{I}, \mathbf{T} | s^*, \Theta^*) \cdot \Pr(n_m | p_m, n_{total}),$$

where

$$n_m \sim \text{Binomial}(n_{total}, p_m).$$

Constraints: Researchers may also make the model identifiable by constraining a model parameter to a known constant value. For example, we impose the constraint $\sigma = 1$ on the gynodioecious model, based on field observations in ???. This reduces Ψ to three dimensions. When a parameter is constrained in this way, it is no longer a free parameter and no longer requires a prior distribution.

One important special case is when τ is constrained to be 1 in the pure hermaphrodite and the androdioecious model. In this case, \tilde{s} becomes identical to s^* . The constrained model may be interpreted as addressing only fraction of uniparental individuals at breeding but not conception. We then write

$$s^* \sim \text{Uniform}(0, 1).$$

Informative priors: Prior knowledge about the values of a parameter may also be incorporated into an analysis by providing an informative prior distribution for that parameter. We use this approach to illustrate the incorporation of additional data on inbreeding depression (τ). While a full treatment of data from greenhouse experiments informative about τ would require the development of a likelihood function that explicitly models the results of those experiments, we here incorporate results reported by Sakai et al. (1989) through a prior distribution:

$$\tau \sim \text{Beta}(2, 8).$$

Required information: When Ψ contains multiple dimensions, additional information about all but one dimension must be included in order to ensure identifiability. This extra information can take the form of additional data, constraints, or informative priors. Information about the remaining dimension is then obtained from the genotypic data \mathbf{X} .

Incorporating information about free parameters of Ψ through the use of informative priors does not make these parameters identifiable, since identifiability is defined in terms of the likelihood, which is unaffected by priors. Incorporating information about parameters in this way is still feasible, since parameters are not required to be identifiable in Bayesian analyses. Nevertheless, we prefer to avoid incorporating data as a prior when possible.

The ability to do inference on parameters that are unidentifiable from the genotypic data \mathbf{X} alone opens exciting new possibilities for inference. For example, given genetic data that are informative about s^* , data on \tilde{s} would allow for the inference of the inbreeding depression τ . Similarly, information on the degree of inbreeding depression would then allow for inference of the fraction of eggs that are self-fertilized. Incorporating additional data in such a flexible fashion is possible because our inference procedure is model-based and relies on a likelihood.

Insufficient information: We recommend using the pure hermaphrodite model constrained so that $\tau = 1$ when there is insufficient information to make the parameters identifiable.

4 Results

4.1 Accuracy and coverage from simulated data

We developed a forward-in-time simulator (<https://github.com/skumagai/selfingsim>) of a pure-hermaphrodite population under the Wright-Fisher model of genetic drift, and generated data under assigned values for effective population size (N), uniparental proportion (s^*), and the locus-specific scaled mutation rates (Θ). We apply our Bayesian method, RMES (David et al., 2007), and the F_{IS} method (Wright, 1969) to simulated data, generated under a known value of s^* . The F_{IS} method uses the observed deficiencies in heterozygotes relative to Hardy-Weinberg proportions, obtaining an estimate of the rate of inbreeding by setting the observed value of F_{IS} equal to its classical expectation $s^*/(2 - s^*)$ (Wright, 1921; Haldane, 1924) and solving for s^* :

$$\hat{s}^* = \frac{2\widehat{F}_{IS}}{1 + \widehat{F}_{IS}}. \quad (24)$$

Appendix C presents a description of the procedures used to assess the accuracy and coverage properties of the three methods.

4.1.1 Accuracy

To assess relative accuracy of estimates of the uniparental proportion s^* , we determine the bias and root-mean-squared error of the three methods by averaging over 10^4 data sets (10^2 independent samples from each of 10^2 independent simulations for each assigned s^*). In contrast with the point estimates of s^* produced by RMES and the F_{IS} method, our Bayesian method generates a posterior distribution. To facilitate comparison, we reduce our estimate to a single value, the median, with the caveat that the mode and mean may show different qualitative behavior (see Appendix C).

Figure 2 indicates that both RMES and our method show positive bias upon application to datasets for which the true uniparental proportion s^* is close to zero and negative bias for s^* close to unity. This trend reflects that both methods yield estimates of s^* constrained to lie

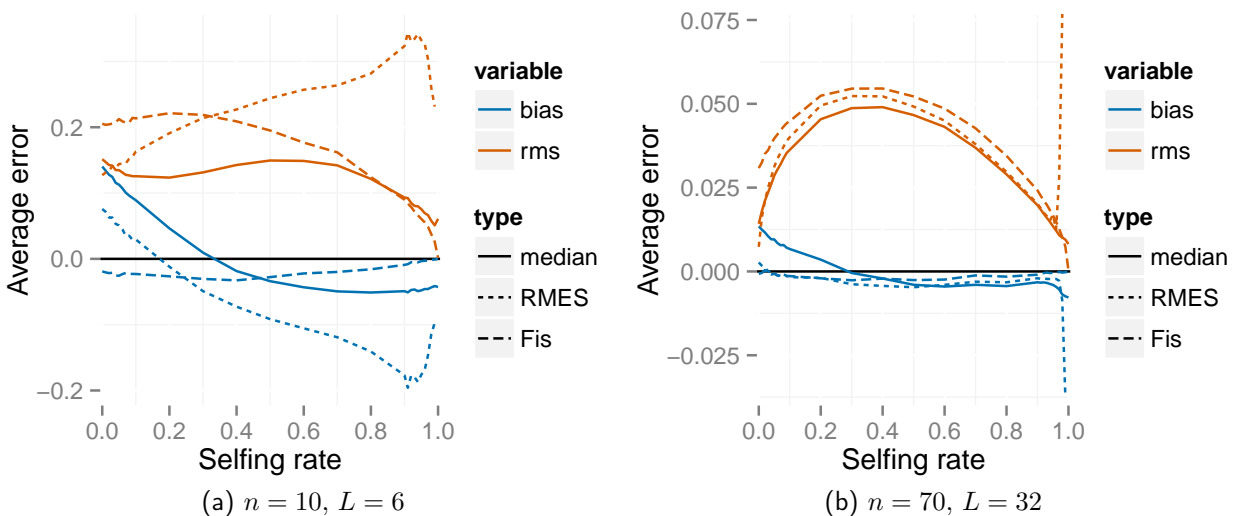


Fig. 2: Errors for the full likelihood (posterior median), RMES, and F_{IS} methods. In the legend, rms indicates the root-mean-squared error and bias the average deviation. Averages are taken across simulated data sets at each true value of s^* .

between 0 and 1. In contrast, the F_{IS} method exhibits negative bias throughout the range. Because the F_{IS} method can produce negative estimates of s^* , this trend is evident even near $s^* = 0$. Our method has a bias near 0 that is substantially larger than the bias of RMES, and an error that is slightly larger. A major contributor to this trend is that our Bayesian estimate is represented by only the median of the posterior distribution of the uniparental proportion s^* . Figure 3 indicates that for datasets generated under a true value of s^* of 0 (full random outcrossing), the posterior distribution for s^* has greater mass near 0. Further, as the posterior mode does not display large bias near 0 (Fig. 20), we conclude that the bias shown by the median (Fig. 2) merely represents uncertainty in the posterior distribution for s^* and not any preference for incorrect values. We note that our method assumes that the data are derived from a population reproducing through a mixture of self-fertilization and

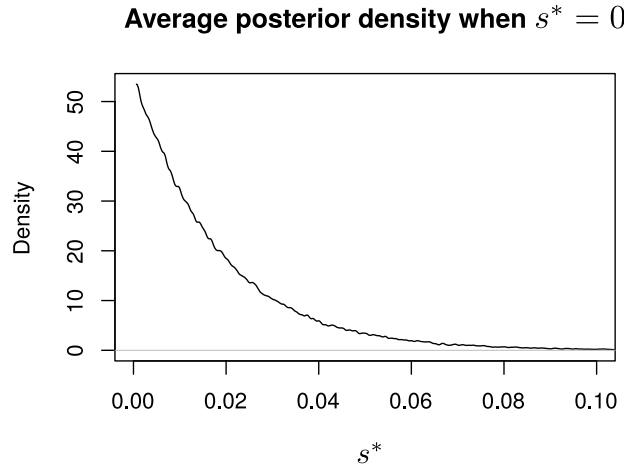


Fig. 3: for $n = 70$, $L = 32$ sampling regime when $s^* = 0$. The average was taken across posterior densities for 100 data sets.

random outcrossing. Assessment of a model of complete random mating ($s^* = 0$) against the present model ($s^* > 0$) might be conducted through the Bayes factor.

Except in cases in which the true s^* is very close to 0, the error for RMES exceeds the error for our method under both sampling regimes (Fig. 2). RMES differs from the other two methods in the steep rise in both bias and rms error for high values of s^* , with the change point occurring at lower values of the uniparental proportion s^* for the small sampling regime ($n = 10$, $L = 6$). A likely contributing factor to the increased error shown by RMES under high values of s^* is the default assumption that the number of generations in the ancestry of any individual does not exceed 20. Violations of this assumption arise more often under high values of s^* , possibly promoting underestimation of the uniparental proportion. Further, RMES discards data at loci at which no heterozygotes are observed, and terminates analysis altogether if the number of loci drops below 2. RMES treats all loci with zero heterozygosity (1) as uninformative, even if multiple alleles are observed. In contrast, our full likelihood method uses data from all loci, with polymorphic loci in the absence of heterozygotes providing strong evidence of high rates of selfing (rather than low rates of mutation). Under the large sampling regime ($n = 70$, $L = 32$), 50% of the loci are discarded on average for true s^* values exceeding 0.94, with less than 10% of data sets unanalyzable (fewer than 2 informative loci) even at $s^* = 0.99$ (Fig. 4). Under the $n = 10$, $L = 6$ regime, 50% of loci are discarded for true s^* values exceeding 0.85, with about 50% of data sets unanalyzable under $s^* \geq 0.94$.

The error for the F_{IS} method also exceeds the error for our method. However, the error for the F_{IS} method is largest near $s^* = 0$ and vanishes as s^* approaches 1.

4.1.2 Coverage

We determine the fraction of data sets for which the confidence interval (CI) generated by RMES and the Bayesian credible interval (BCI) generated by our method contains the true value of the uniparental proportion s^* . This measure of coverage is a frequentist notion, as it treats each true value of s^* separately. A 95% CI should contain the truth 95% of the

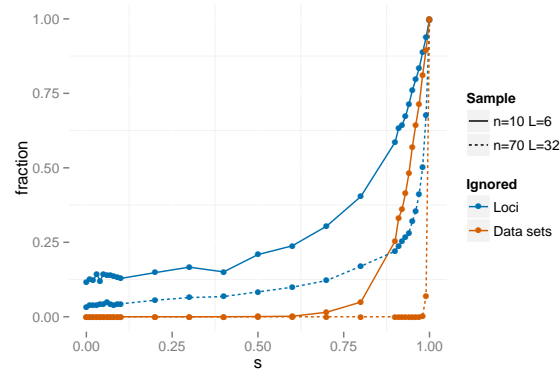


Fig. 4: Fraction of loci and data sets that are ignored by RMES.

time for each specific value of s^* . However, a 95% BCI is not expected to have 95% coverage at each value of s^* , but rather 95% coverage averaged over values of s^* sampled from the prior. Of the various ways to determine a BCI for a given posterior distribution, we choose to report the highest posterior density BCI (rather than the central BCI, for example).

Figure 5 indicates that coverage of the 95% CIs produced by RMES are consistently lower than 95% across all true s^* values under the large sampling regime ($n = 70, L = 32$). Coverage appears to decline as s^* increases, dropping from 86% for $s^* = 0.1$ to 64% for $s^* = 0.99$. In

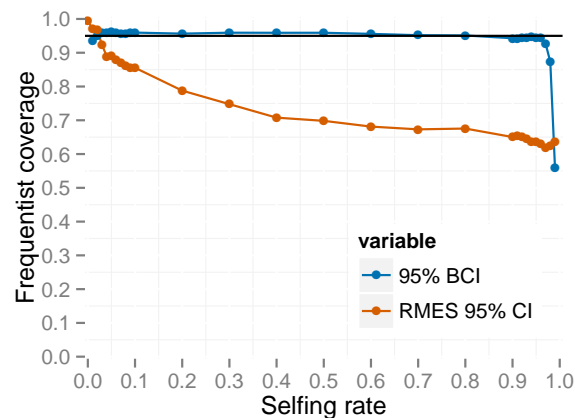


Fig. 5: Frequentist coverage at each level of s^* for 95% intervals from RMES and the method based on the full likelihood under the large sampling regime ($n = 70, L = 32$). RMES intervals are 95% confidence intervals computed via profile likelihood. Full likelihood intervals are 95% HPD Bayesian credible intervals.

contrast, the 95% BCIs have slightly greater than 95% frequentist coverage for each value of s^* , except for s^* values very close to the extremes (0 and 1). Under very high rates of inbreeding ($s^* \approx 1$), an assumption (9) of our underlying model (reproduction occurs on a timescale much shorter than the timescales of mutation and coalescence) is likely violated.

Figure 6 indicates that BCIs of different nominal values (0.5, 0.75, 0.9, 0.95, and 0.99) display the same pattern, with coverage exceeding the desired value for intermediate true s^*

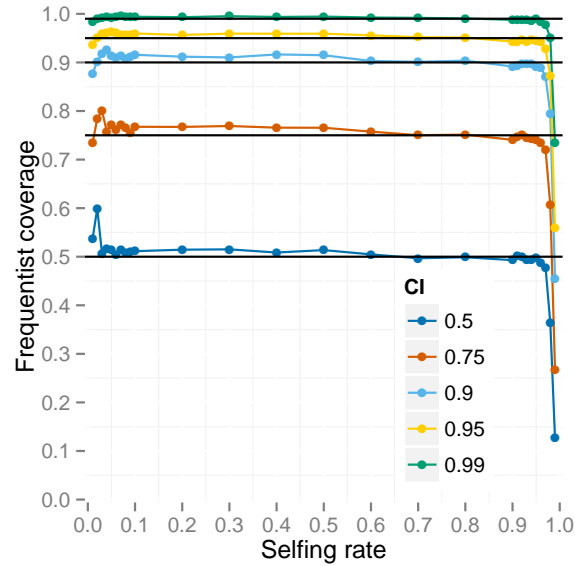


Fig. 6: Frequentist coverage for Bayesian credible intervals at different levels of credibility under the large sampling regime ($n = 70, L = 32$).

values and dipping below the desired value for very high values of s^* . Coverage is closer to the nominal value for the 0.99 and 0.95 levels than for the 0.5 level.

4.1.3 Distribution of selfing generations

In order to check the accuracy of our reconstructed generations of selfing, we examine the posterior distributions of selfing times $\{T_k\}$ for $s^* = 0.5$ under the large sampling regime ($n = 70, L = 32$). We average posterior distributions for selfing times across 100 simulated

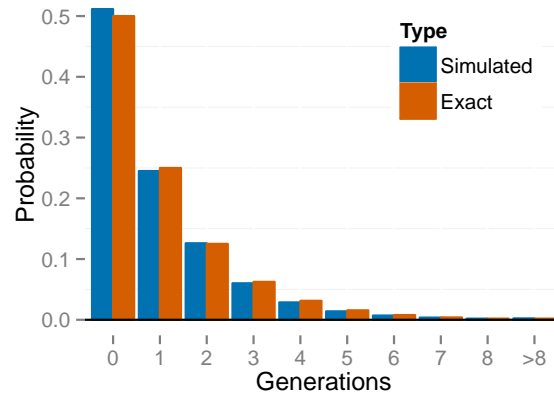


Fig. 7: times under $s^* = 0.5$ compared to the posterior distribution averaged across individuals and across data sets.

data sets, and across individuals $k = 1 \dots 70$ within each simulated data set. We then

compare these averages based on the simulated data with the exact distribution of selfing times across individuals (Figure 7). The pooled posterior distribution closely matches the exact distribution. This simple check suggests that our method correctly infers the true posterior distribution of selfing times for each sampled individual.

4.2 Analysis of microsatellite data derived from an androdioecious vertebrate

We begin by examining 32-locus microsatellite genotypes ascertained in the mangrove killifish *Kryptolebias marmoratus* (Tatarenkov et al., 2007). This organism, comprising hermaphrodites and males, is virtually unique among vertebrates in reproducing routinely by self-fertilization. We apply our method under the androdioecious model, incorporating data on the number of observed males in addition to the array of microsatellite genotypes. we model the n_m males observed in a sample of n_{total} fish as a binomial random variable:

$$n_m \sim \text{Binomial}(n_{total}, p_m), \quad (25)$$

for p_m the proportion of males in the population, we obtain an extended likelihood by multiplying the likelihood for the genetic data by $\Pr(n_m | n_{total}, p_m)$. Our method simultaneously estimates the proportion of males in the population (p_m) together with rates of locus-specific mutation (θ^*) and the uniparental proportion (s^*). We apply the method to two populations, which show highly divergent rates of inbreeding.

4.2.1 BP population

We applied our method to the BP dataset described by Tatarenkov et al. (2012). This dataset comprises a total of 70 individuals, collected in 2007, 2010, and 2011 from the Big Pine location on the Florida Keys.

Tatarenkov et al. (2012) report 21 males among the 201 individuals collected from various locations in the Florida Keys during this period, consistent other estimates of about 1% (*e.g.*, Turner et al., 1992). Based on the long-term experience of the Tatarenkov–Avisé laboratory with this species, we assumed observation of $n_m = 20$ males out of $n_{total} = 2000$ individuals in (25). We estimate that the fraction of males in the population (p_m) has a posterior median of 0.01 with a 95% Bayesian Credible Interval (BCI) of (0.0062, 0.015).

Our estimates of mutation rates (θ^*) indicate substantial variation among loci, with the median ranging from about 0.5 to about 5 (Fig. 8). The distribution of mutation rates across loci appears to be multimodal, with many loci having a relatively low rate and a few having larger rates.

Figure 9 shows the posterior distribution of uniparental proportion s^* , with a median of 0.95 and a 95% BCI of (0.93, 0.97)). This estimate is somewhat lower than the F_{IS} method estimate of 0.97, and slightly higher than the RMES estimate of 0.94, which has a 95% Confidence Interval (CI) of (0.91, 0.96). We note that RMES discarded from the analysis 9 loci (out of 32) which showed no heterozygosity, even though 7 of the 9 were polymorphic in the sample.

We also estimate the posterior distribution of selfing times for each individual, and display them in Figure 10. Figure 11 shows the empirical distribution of the selfing time T across

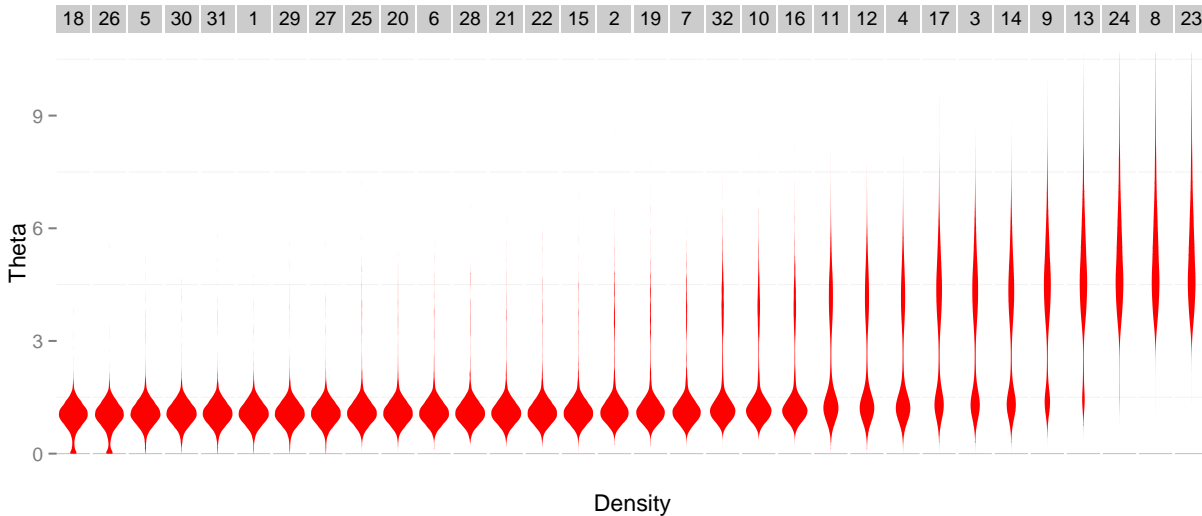


Fig. 8: Posterior distributions for mutation rates at each locus in *K. marmoratus* (BP population). The locus for each distribution is indicated by the grey shaded box above.

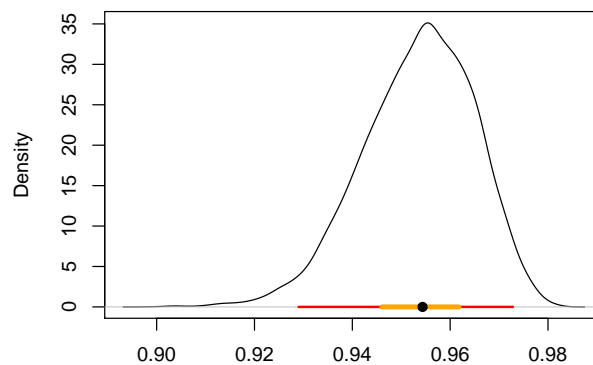


Fig. 9: Posterior distribution of the uniparental proportion s^* for the BP population. The median is indicated by a black dot, with a red bar for the 95% BCI and an orange bar for the 50% BCI.

individuals, averaged over posterior uncertainty.

These figures indicate a complete absence of individuals predicted to have 0 generations of selfing. This indicates that individuals with 0 generations of selfing (i.e. out-crossed individuals) have less heterozygosity than predicted in a model based on selfing and panmixia alone. Out-crossed individuals thus are estimated to have undergone 1 or 2 generations of selfing. This lack of heterozygosity even among out-bred individuals suggests that population subdivision or bi-parental inbreeding may be responsible.

4.2.2 TC population

We applied our method to the sample collected in 2005 from Twin Cays, Belize (TC05, Mackiewicz et al., 2006). Several attributes of this population depart sharply from the BP population (preceding section), including a much higher incidence of males and much higher

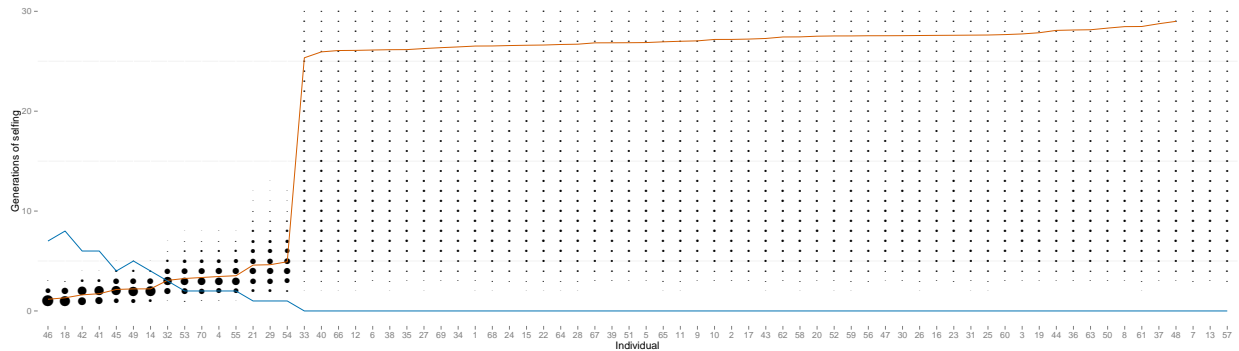


Fig. 10: Estimated number of selfing generations for each individual for *K. marmoratus* (BP population). The area of each dot indicates the posterior probability that a numbered individual (x-axis) has been selfed for a given number of generations (y-axis). For each individual the blue line indicates the posterior mean number of selfing generations and the red line indicates the number of heterozygous loci. The y-axis is truncated to $[0, 30]$.

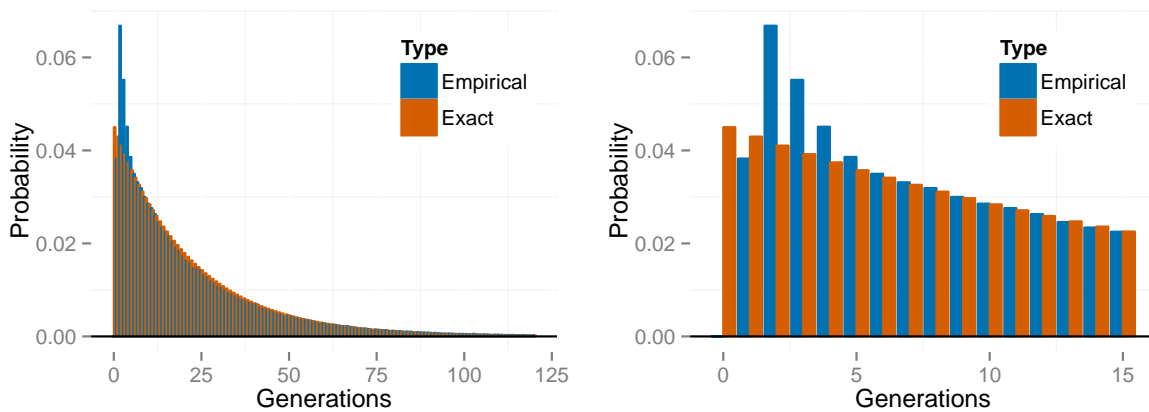


Fig. 11: Empirical distribution of selfing times T across individuals, for *K. marmoratus* (Population BP). The histogram is averaged across posterior samples. The right panel is constructed by zooming in on the panel on the left. The first bar with positive probability is for $T = 1$.

polymorphism and heterozygosity.

We incorporated the observation of 19 males among the 112 individuals collected from Belize in 2005 (Mackiewicz et al., 2006) into the likelihood (see (25)). Our estimate of the fraction of males in the population (p_m) has a posterior median of 0.17 with a 95% BCI of (0.11, 0.25).

Figure 12 presents posterior distributions of locus-specific mutation rates, with medians

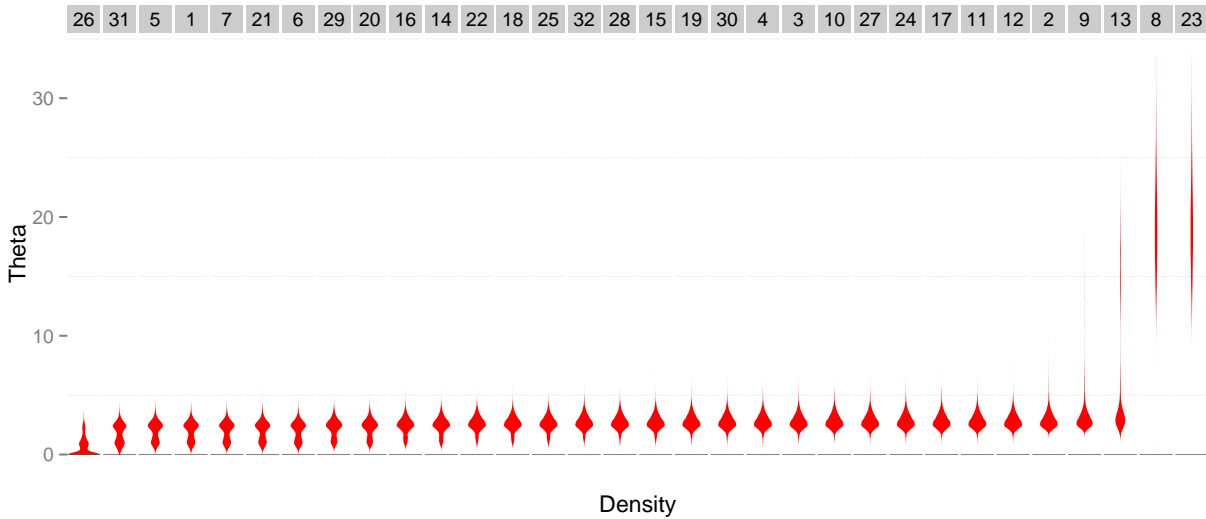


Fig. 12: Mutation rates at each locus for *K. marmoratus* (TC population). The locus for each distribution is indicated by the grey shaded box above.

ranging from about 0.5 to about 23. As for the BP population, most loci appear to have a relatively low mutation rate, with a substantially higher mutation rate shown by two loci (both of which appear to have a high rate in the BP population as well).

All three methods confirm the inference of Mackiewicz et al. (2006) of much lower inbreeding in the TC population relative to the BP population. Our posterior distribution of uniparental proportion s^* has a median and 95% BCI of 0.35 (0.25, 0.45) (Fig. 13). The

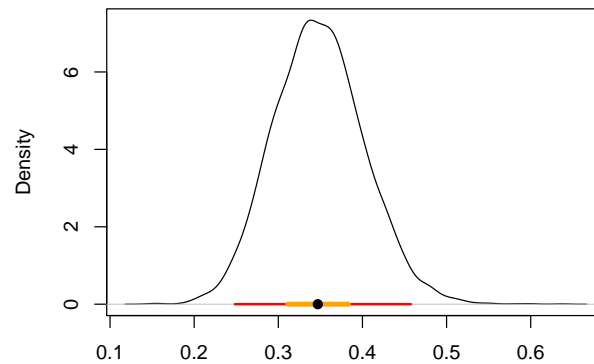


Fig. 13: Posterior distribution of the uniparental proportion s^* for the TC population. Also shown are the 95% BCI (red), 50% BCI (orange), and median (black dot).

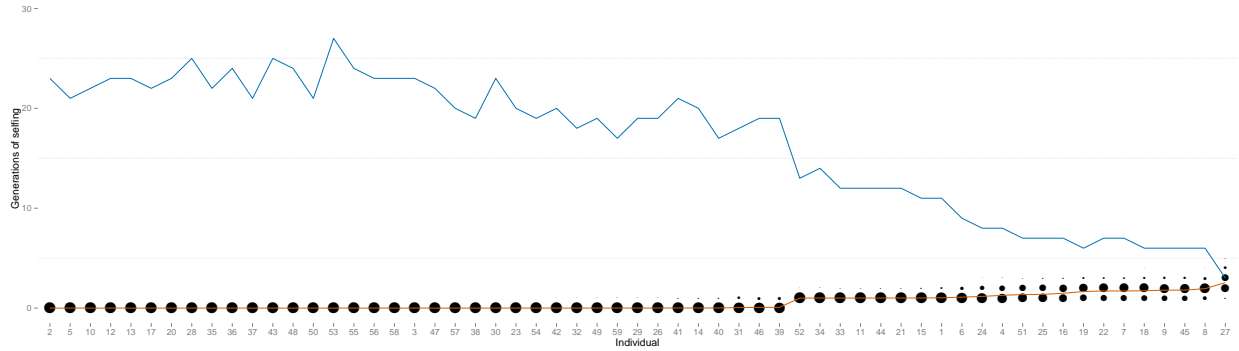


Fig. 14: Estimated number of selfing generations for each individual for *K. marmoratus* (TC population). Each dot indicates the posterior probability that a numbered individual (x-axis) has been selfed for a given number of generations (y-axis). For each individual the blue line indicates the posterior mean number of selfing generations and the red line indicates the number of heterozygous loci.

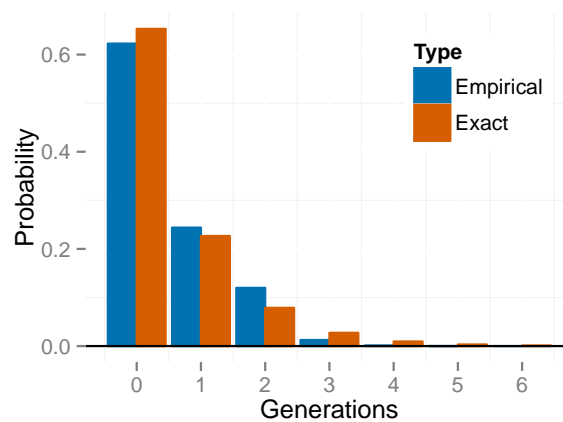


Fig. 15: Empirical distribution of selfing times T across individuals, for *K. marmoratus* (Population TC). The histogram is averaged across posterior samples.

median again lies between the F_{IS} estimate of 0.39 and the RMES estimate of 0.33, with a 95% CI of (0.30, 0.36). In this case, RMES excluded from the analysis only a single locus, which was monomorphic in the sample.

Figure 14 presents the posterior distribution of the number of consecutive generations of selfing in the immediate ancestry of each individual. Figure 15 shows the empirical distribution of the selfing time T across individuals, averaged over posterior uncertainty. In contrast to the previous population, this population does not seem to have significant sources of inbreeding that are not explained by selfing.

4.3 Analysis of microsatellite data derived from a gynodioecious plant

We next examine data from *Schiedea salicaria*, a gynodioecious member of the carnation family endemic to the Hawaiian islands. We analyzed genotypes at 9 microsatellite loci from 25 *S. salicaria* individuals collected from west Maui and identified by Wallace et al. (2011) as non-hybrids. Campbell et al. (2010) reported a 12% proportion of females (27 females among 221 individuals). In addition, we place an informative prior on the relative viability of inbred individuals,

$$\tau \sim \text{Beta}(2, 8),$$

the mean of which (0.2) is consistent with the results of greenhouse experiments reported by Sakai et al. (1989).

Estimates of the locus-specific mutation rate do not indicate substantial evidence for differences in mutation rate across loci, with posterior medians close to 1 for all loci (Figure 16).

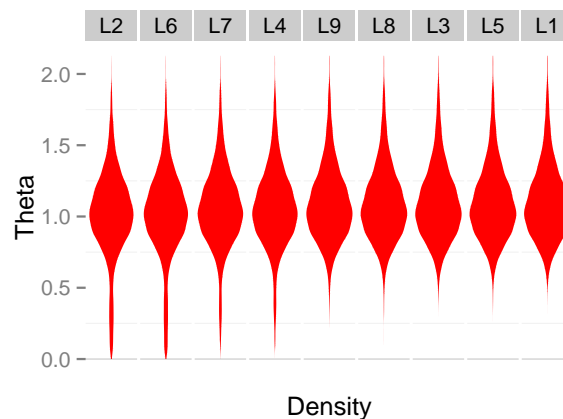


Fig. 16: Posterior distributions for mutation rates at locus in *S. salicaria*. The locus for each distribution is indicated by the grey shaded box above.

The fraction of selfed seeds a has a posterior median of 0.695 and a 95% BCI of (0.299, 0.971). The selfing rate s^* has a posterior median of 0.247 and a 95% BCI of (.0791, 0.444). This is substantially lower than the F_{IS} method's estimate of $s^* = 0.33$. RMES, on the other hand, gives an estimate of 0, with a 95% CI of (0, 0.15). No loci were excluded by RMES. We also estimate the selfing times for each individual, and display them in figure 18. Figure 19 shows the empirical distribution of the selfing time T across individuals, averaged over posterior uncertainty.

Posterior medians and 95% BCIs for a , s^* , τ , and p_f are given in Table 1 (Figure 17).

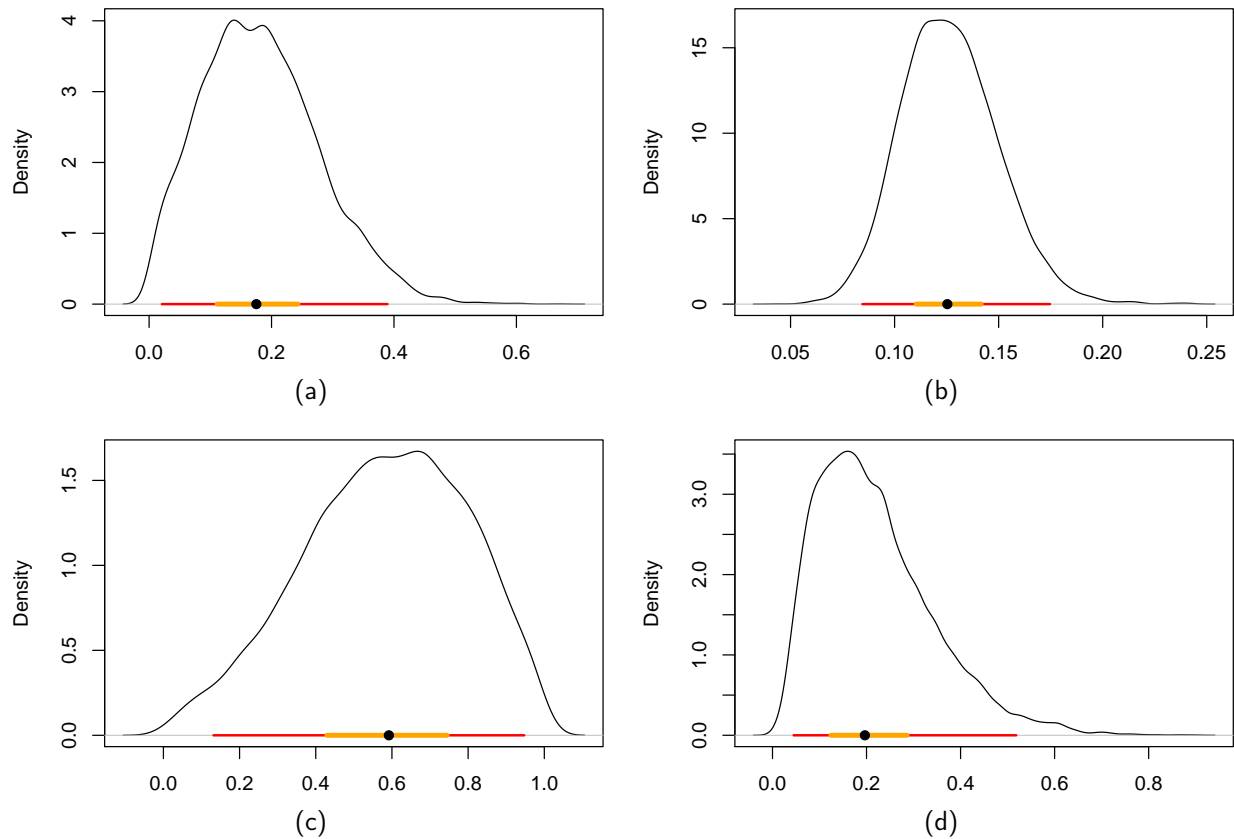


Fig. 17: Posterior distributions on (a) s^* , (b) p_f , (c) a , and (d) τ for *Schiedea salicaria*. Also shown are 95% BCI (red), 50% BCI (orange), and median (black dot).

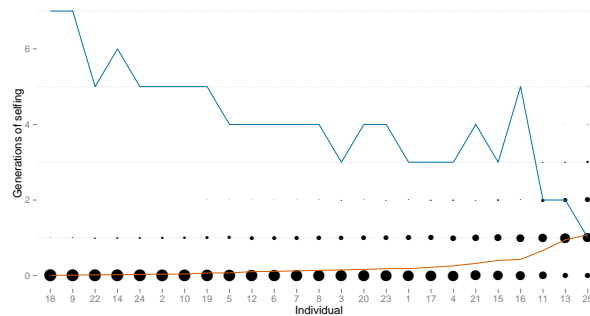


Fig. 18: Estimated number of selfing generations for each individual for *S. salicaria*. The area of each dot indicates the posterior probability that a numbered individual (x-axis) has been selfed for a given number of generations (y-axis). For each individual the blue line indicates the posterior mean number of selfing generations and the red line indicates the number of heterozygous loci.

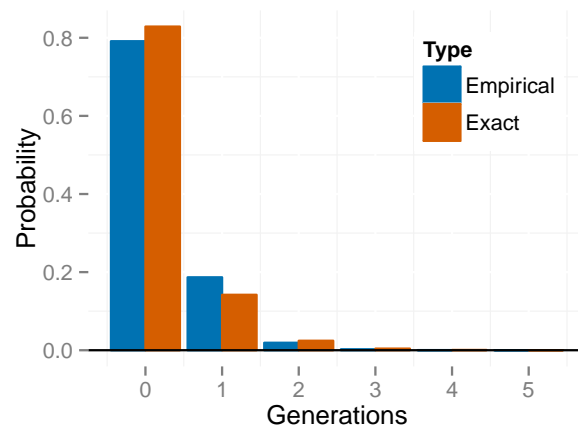


Fig. 19: Empirical distribution of selfing times T across individuals, for *S. salicaria*. The histogram is averaged across posterior samples.

Tab. 1: Parameter estimates for different amounts of data. Estimates are given by a posterior median and a 95% BCI.

G	F	I	a	s^*	τ	p_f	C
Y	Y	Y	0.695 (0.299, 0.971)	0.247 (0.0791, 0.444)	0.215 (0.0597, 0.529)	0.125 (0.0849, 0.173)	1.01 (1, 1.22)
Y	Y	N	0.497 (0.187, 0.93)	0.267 (0.0951, 0.469)	0.507 (0.082, 0.973)	0.125 (0.0851, 0.174)	1.02 (1, 1.1)
N	Y	Y	0.496 (0.0252, 0.974)	0.112 (0.0026, 0.588)	0.183 (0.0277, 0.513)	0.125 (0.0847, 0.173)	1.02 (1, 1.14)
N	Y	N	0.504 (0.025, 0.973)	0.231 (0.00391, 0.776)	0.493 (0.0257, 0.975)	0.125 (0.0847, 0.173)	1.02 (1, 1.06)
N	N	N	0.497 (0.0244, 0.975)	0.0844 (0.000797, 0.643)	0.494 (0.0252, 0.975)	0.479 (0.0245, 0.972)	1.17 (1, 9.52)

Each row represents an analysis that includes (Y) or excludes (N) various sources of information. G indicates genotypic data, F indicates data about the frequency of females, and I indicates the use of the informative prior on τ as opposed to a Uniform(0,1) prior. The bottom row of the table indicates that the induced prior distribution on the composite parameter s^* is not Uniform(0,1), since the prior estimate for s^* is 0.0844 (0.000797, 0.643). By comparing the first and third rows, we can see that inclusion of the genetic data shifts the posterior median of s^* from 0.112 to 0.247, as well as shrinking the width of the credible interval.

5 Discussion

We introduce a model-based Bayesian method for the inference of rates of self-fertilization and other aspects of a mixed mating system. Designed to accommodate large (even genome-scale) numbers of loci, it uses the Ewens Sampling Formula (ESF) to determine likelihoods in a computationally efficient manner from frequency spectra of genotypes observed at multiple unlinked sites throughout the genome. Tests using simulated data suggest that the method provides both accurate estimates of selfing rates and accurate assessments of uncertainty.

5.1 Assessment of the new approach

Accuracy: Enjalbert and David (2000) and David et al. (2007) base estimates of selfing rate on the distribution of numbers of heterozygous loci. Both methods strip genotype information from the data, distinguishing between only homozygotes and heterozygotes, irrespective of the alleles involved. Loci lacking heterozygotes altogether (even if polymorphic) are removed from the analysis as uninformative about the magnitude of departure from Hardy-Weinberg proportions (Fig. 4). As the observation of polymorphic loci with low heterozygosity provides strong evidence of inbreeding, exclusion of such loci from **RMES** (David et al., 2007) analyses may contribute to its loss of accuracy for high rates of selfing (Fig. 2).

Our method derives information from all loci. Like most coalescence-based models, it accounts for the level of variation as well as the way in which variation is partitioned within the sample. Even a locus monomorphic within a sample provides information about the age of the most recent common ancestor of the observed sequences, a property that was not widely appreciated prior to analyses of the absence of variation in a sample of human Y chromosomes (Dorit et al., 1995; Fu and Li, 1996).

Estimates of the rate of inbreeding produced by our method appear to show greater accuracy than **RMES** and the F_{IS} method over much of the parameter range (Fig. 2). The increased error exhibited under very high rates of inbreeding ($s^* \approx 1$) may reflect violation of our assumption (9) that out-breeding occurs on a much shorter timescale than mutation and coalescence. Even though our method assumes that the rate of inbreeding lies in $(0, 1)$, the posterior distribution for data generated under random outcrossing ($s^* = 0$) does indicate greater confidence in low rates of inbreeding (Fig. 3).

Both **RMES** (David et al., 2007) and our method invoke independence of genealogical histories of unlinked loci, conditional on the time since the most recent outcrossing event. **RMES** seeks to approximate the likelihood by summing over the distribution of time since the most recent outcross event, but truncates the infinite sum at 20 generations. The increased error exhibited by **RMES** under high rates of inbreeding may reflect that the likelihood has a substantial mass beyond the truncation point in such cases. Our method explicitly estimates the latent variable of time since the most recent outcross for each individual (13). This quantity ranges over the non-negative integers, but values assigned to individuals are explored by the MCMC according to their effects on the likelihood.

Frequentist coverage properties: Bayesian approaches afford a direct means of assessing confidence in parameter estimates, and our simulation studies suggest that the Bayesian

Credible Intervals (BCIs) generated by our method have relatively good frequentist coverage properties as well (Fig. 6). The Confidence Intervals (CIs) reported by the maximum-likelihood method **RMES** (David et al., 2007) appear to perform less well (Fig. 5). **RMES** determines CIs via the profile likelihood method. However, when determining the likelihood profile for s^* **RMES** holds other parameters constant instead of reoptimizing them to maximize the likelihood as s^* varies. The result is therefore not a true profile likelihood, which may explain the poor coverage properties of the CIs that **RMES** provides (Kreutz et al., 2013).

Model fit: Bayesian approaches also afford insight into the suitability of the underlying model. Our method provides estimates of the number of generations since the most recent outcross event in the immediate ancestry of each individual (T). We can pool such estimates of selfing times to obtain an empirical distribution of the number of selfing generations, a procedure particularly useful for samples containing observation of the genotype of many individuals. Under the assumption of a single population-wide rate of self-fertilization, we expect the selfing time to have a geometric distribution with parameter corresponding to the estimated selfing rate (Fig. 7). Empirical distributions of the estimated number of generations since the last outcross appear consistent with this expectation for the TC *K. marmoratus* population (Fig. 15) and for Schiedea (Fig. 19). In contrast, the empirical distribution for the highly-inbred BP *K. marmoratus* population (Fig. 11) shows an absence of individuals formed by random outcrossing ($T = 0$). This discrepancy may indicate a departure from the underlying model, which assumes reproduction either through self-fertilization or through random outcrossing. In particular, high rates of biparental inbreeding as well as selfing may reduce the fraction of individuals formed by random outcrossing. Mis-scoring of heterozygotes as homozygotes due to null alleles or other factors, a possibility directly addressed by **RMES** (David et al., 2007), may in principle contribute to the paucity of outbred individuals as well.

5.2 Components of inference

Locus-specific mutation rates: Our method estimates scaled mutation rates at each locus using the DPP. This approach improves on existing methods in several ways. First, we estimate a single parameter at each locus instead of estimating a large number of allele frequencies like Enjalbert and David (2000). This improves the accuracy of the estimates. Second, we estimate mutation rates instead of the heterozygosity (1) at each site. The mutation rate is more desirable to estimate, since it characterizes the evolutionary process itself as opposed to a random outcome. Third, we further improve accuracy by use of the DPP. The DPP allows us to estimate the number of classes of mutation rates, the mutation rate for each class, and the class membership of each locus. The DPP therefore gives us the increased accuracy of pooling similar sites without the requirement to know *a priori* which sites are similar, or even the number of classes.

Distinguishing between rates of mutation and inbreeding: The Ewens Sampling Formula (ESF, Ewens, 1972) provides the probability, under the infinite-alleles model of mutation, of an allele frequency spectrum (AFS) observed at a locus in a sample derived from a

panmictic population. Under partial-self-fertilization, the ESF provides the probability of the AFS observed in a sample of genes, each taken from a distinct individual. For such genic (as opposed to genotypic) samples, the coalescence process under inbreeding is identical to the standard coalescence process, but with a rescaling of time (Fu, 1997; Nordborg and Donnelly, 1997). Accordingly, genic samples may serve as the basis for the estimation of the single parameter of the ESF, the scaled mutation rate θ^* (10), but not the rate of inbreeding apart from the scaled mutation rate.

Our method uses the information in a genotypic sample, the genotype frequency spectrum, to infer both the uniparental proportion s^* and the scaled mutation rate θ^* . All loci within a randomly sampled individual share a common history of inbreeding back to the most recent random outcross event. Even in the absence of physical linkage, this common history generates identity disequilibrium (Cockerham and Weir, 1968), the correlation in heterozygosity across loci. The number of consecutive generations of inbreeding in the immediate ancestry of a given individual (T_k for individual k) corresponds to a latent variable in our Bayesian inference framework. The probability of the heterozygosity profile of individual k depends on T_k which in turn depends on the rate of inbreeding (15). Observation of multiple individuals provides a basis for the estimation of the uniparental proportion s^* as well as the scaled mutation rate θ^* .

5.3 Comprehensive characterization of mating systems

Incorporating additional data: In the absence of information beyond the genotype frequency spectrum observed in a sample, the likelihood depends on just two composite parameters: the probability that a random individual is uniparental (s^*) and the scaled rate of mutation θ^* (10). In addressing pure hermaphroditism, androdioecy, and gynodioecy, we have determined the dependence of these composite parameters on various biological aspects (Section 2.1 and Appendix A). For example, the gynodioecy model includes the viability of inbred offspring relative to outbred offspring, the proportion of hermaphrodites among reproductives, and the rate of seed set by male-steriles (females) relative to hermaphrodites. Using the genotype frequency spectrum observed in a sample alone, such basic parameters are nonidentifiable: any set that determine the same values of composite parameters s^* and θ^* have the same likelihood.

Extended likelihoods: Incorporating information beyond the genotypic frequency spectrum affords insight into the basic parameters. In our analysis of microsatellite data from the killifish *K. marmoratus*, for example, counts of males and hermaphrodites observed in the population provide information about the relative rate of coalescence C (8) apart from the scaled rate of mutation θ^* (10).

Our implementation of our inference method explicitly incorporates the full set of parameters for each mating system. By allowing inference on possibly nonidentifiable parameters, this feature introduces the possibility of using information of various kinds in addition to the genotype data. In particular, incorporation of observations on the proportions of males and hermaphrodites into our analysis of the *K. marmoratus* data permitted the joint estimation of the uniparental fraction s^* and the proportion of males. Empirical data on the intensity of inbreeding depression would permit inference of the proportion of self-fertilization events.

Our analysis of gynodioecious *Schiedea* introduced previous experimental results on inbreeding depression through the prior distribution for the relative viability of inbred offspring (τ), permitting inference about the fraction of seeds of hermaphrodites that are set by self-pollen (Table 1). A comprehensive analysis, incorporating a joint likelihood across multiple kinds of observations, would allow characterization of various aspects of the mating system in addition to the rate of self-fertilization.

Acknowledgments

We thank Lisa E. Wallace and Theresa M. Culley for making available to us the microsatellite data from *Schiedea salicaria*. Public Health Service grant GM 37841 (MKU) provided partial funding for this research.

References

- Ayres KL, Balding DJ. 1998. Measuring departures from Hardy-Weinberg: a Markov chain Monte Carlo method for estimating the inbreeding coefficient. *Heredity*. 80:769–777.
- Campbell DR, Weller SG, Sakai AK, Culley TM, Dang PN, Dunbar-Wallis AK. 2010. Genetic variation and covariation in floral allocation of two species of *Schiedea* with contrasting levels of sexual dimorphism. *Evolution*. 65:757–770.
- Clegg MT. 1980. Measuring plant mating systems. *Bioscience*. 30:814–818.
- Cockerham CC, Weir BS. 1968. Sib mating with two linked loci. *Genetics*. 60:629–640.
- David P, Pujol B, Viard F, Castella V, Goudet J. 2007. Reliable selfing rate estimates from imperfect population genetic data. *Mol Ecol*. 16:2474–2487.
- Dorit RL, Akashi H, Gilbert W. 1995. Absence of polymorphism at the ZFY locus on the human Y chromosome. *Science*. 286:1183–1185.
- Enjalbert J, David JL. 2000. Inferring recent outcrossing rates using multilocus individual heterozygosity: application to evolving wheat populations. *Genetics*. 156:1973–1982.
- Ewens WJ. 1972. The sampling theory of selectively neutral alleles. *Theoretical population biology*. 3:87–112.
- Fu YX. 1997. Coalescent theory for a partially selfing population. *Genetics*. 146:1489–1499.
- Fu YX, Li WH. 1996. Absence of polymorphism at the ZFY locus on the human Y chromosome. *Science*. 272:1356–1357.
- Gao H, Williamson S, Bustamante CD. 2007. A markov chain monte carlo approach for joint inference of population structure and inbreeding rates from multilocus genotype data. *Genetics*. 176:1635–1651.

- Haldane J. 1924. A mathematical theory of natural and artificial selection. part ii the influence of partial self-fertilisation, inbreeding, assortative mating, and selective fertilisation on the composition of mendelian populations, and on natural selection. *Biological Reviews*. 1:158–163.
- Hill WG, Babiker HA, Ranford-Cartwright LC, Walliker D. 1995. Estimation of inbreeding coefficients from genotypic data on multiple alleles, and application to estimation of clonality in malaria parasites. *Genet. Res.* 65:53–61.
- Karlin S, McGregor J. 1972. Addendum to a paper of w. ewens. *Theoretical Population Biology*. 3:113–116.
- Kreutz C, Raue A, Kaschek D, Timmer J. 2013. Profile likelihood in systems biology. *FEBS Journal*. 280:2564–2571.
- Mackiewicz M, Tatarenkov A, Taylor DS, Turner BJ, Avise JC. 2006. Extensive outcrossing and androdioecy in a vertebrate species that otherwise reproduces as a self-fertilizing hermaphrodite. *Proc Natl Acad Sci U S A*. 103:9924–9928.
- Nordborg M, Donnelly P. 1997. The coalescent process with selfing. *Genetics*. 146:1185–1195.
- Pritchard JK, Stephens M, Donnelly P. 2000. Inference of population structure using multilocus genotype data. *Genetics*. 155:945–959.
- Ritland K. 2002. Extensions of models for the estimation of mating systems using n independent loci. *Heredity*. 88:221–228.
- Sakai AK, Karoly K, Weller SG. 1989. Inbreeding depression in *Schiedea globosa* and *S. salicaria* (Caryophyllaceae), subdioecious and gynodioecious Hawaiian species. *American Journal of Botany*. pp. 437–444.
- Tatarenkov A, Earley RL, Taylor DS, Avise JC. 2012. Microevolutionary distribution of isogenicity in a self-fertilizing fish (*Kryptolebias marmoratus*) in the Florida Keys. *Integr. Comp. Biol.* 52:743–752.
- Tatarenkov A, Gao H, Mackiewicz M, Taylor DS, Turner BJ, Avise JC. 2007. Strong population structure despite evidence of recent migration in a selfing hermaphroditic vertebrate, the mangrove killifish (*kryptolebias marmoratus*). *Mol Ecol*. 16:2701–2711.
- Turner BJ, Davis WP, Taylor DS. 1992. Abundant males in populations of a selfing hermaphrodite fish, *Rivulus marmoratus*, from some Belize cays. *J. Fish Biol.* 40:307–310.
- Wallace LE, Culley TM, Weller SG, Sakai AK, Kuenzi A, Roy T, Wagner WL, Nepokroeff M. 2011. Asymmetrical gene flow in a hybrid zone of Hawaiian *Schiedea* (Caryophyllaceae) species with contrasting mating systems. *PLoS ONE*. 6:e24845. Doi:10.1371/journal.pone.0024845.

Wang J, EL-KASSABY YA, Ritland K. 2012. Estimating selfing rates from reconstructed pedigrees using multilocus genotype data. *Molecular ecology*. 21:100–116.

Wright S. 1921. Systems of mating. I, II, III, IV, V. *Genetics*. 6:111–178.

Wright S. 1969. *Evolution and the Genetics of Populations, Vol. 2, The Theory of Gene Frequencies*. Chicago: Univ. Chicago Press.

A Uniparental proportion and rate of parent-sharing

For the mating systems of pure hermaphroditism, androdioecy, and gynodioecy, we provide expressions for the probability that a random individual is uniparental (s^*) and the probability that a pair of genes sampled from distinct individuals derive from the same individual in the immediately preceding generation ($1/N^*$).

A.1 Pure hermaphroditism

Each generation, N_h reproductives generate offspring, of which a proportion \tilde{s} at conception are uniparental.

Uniparental proportion: We assume that the magnitude of inbreeding or outbreeding depression depends only on the reproductive mode through which offspring are derived. The probability that a random individual is uniparental (s^*) corresponds to the fraction of uniparentals among surviving offspring:

$$s_H = \frac{\tilde{s}\tau}{\tilde{s}\tau + 1 - \tilde{s}}$$

(see (2a)), for τ the rate of survival of a uniparental zygote relative to a biparental zygote.

Parent-sharing: We address $1/N^*$, the probability that two genes, each sampled from a random individual, derive from the same individual in the immediately preceding generation. In the case in which the individuals bearing the sampled genes are both uniparental (probability s_H^2), they share their parent with probability $1/N_h$ and the pair of genes are derived from that parent with probability 1. For genes sampled from two biparental individuals (probability $(1 - s_H)^2$), the individuals share exactly 1 parent with probability

$$\frac{\binom{2}{1}\binom{N_h-2}{1}}{\binom{N}{2}} = \frac{4}{N_h} + o\left(\frac{1}{N_h}\right),$$

and 2 parents with a probability of smaller order. Both genes derive from the common parent with probability $1/4$. In the remaining case (genes from a uniparental and a biparental individual), the individuals share a parent with probability

$$\frac{\binom{1}{1}\binom{N_h-1}{1}}{\binom{N_h}{2}} = \frac{2}{N_h},$$

and both genes derive from that parent with probability $1/2$.

We address the probability that two genes, each sampled from a random individual, derive from the same individual in the immediately preceding generation. In the case in which the individuals bearing the sampled genes are both uniparental (probability s_H^2), they share their parent with probability $1/N_h$ and the pair of genes are derived from that parent with probability 1. For a pair of genes pair both sampled from biparental individuals (probability $(1 - s_H)^2$), they share their parent with probability $1/N_h$ and the pair of genes are derived from that parent with probability 1.

To order $1/N_h$, the total probability that a pair of genes sampled from distinct individuals derive from the same parent ($1/N^*$) is given by (2b):

$$1/N_H = [s_H^2 + 4s_H(1 - s_H)(1/2) + 4(1 - s_H)^2(1/4)] / N_h = 1/N_h.$$

For this model, we assign the arbitrary constant N in (8) as N_h , implying $C = 1$.

A.2 Androdioecy

The reproductive population comprises N_h hermaphrodites and N_m males. A proportion \tilde{s} of broods derive from self-fertilization and the complement from fertilization by males.

Uniparental proportion: The proportion (s^*) of individuals that are uniparental (3a) is identical to the case of pure hermaphroditism (2a).

Parent-sharing: Under androdioecy, all maternal parents are hermaphroditic. A pair of uniparental individuals share their parent with probability

$$\frac{1}{N_h}. \quad (\text{A.1a})$$

A uniparental individual and a biparental individual share a parent with this probability as well. A pair of biparental individuals share their maternal parent but not their paternal parent with probability

$$\frac{N_m - 1}{N_h N_m}, \quad (\text{A.1b})$$

and only their paternal parent with probability

$$\frac{N_h - 1}{N_h N_m}. \quad (\text{A.1c})$$

Assuming negligible probabilities of sharing of more than one parent by two offspring or sharing of a parent by more than two offspring, we obtain the probability (3b) that a pair of genes sampled from distinct individuals derive from the same parent ($1/N^*$):

$$\begin{aligned} \frac{1}{N_A} &= s_A^2 \frac{1}{N_h} + 2s_A(1 - s_A) \frac{1}{2N_h} + (1 - s_A)^2 \left(\frac{1}{4N_h} + \frac{1}{4N_m} \right) \\ &= \frac{(1 + s_A)^2}{4N_h} + \frac{(1 - s_A)^2}{4N_m}. \end{aligned}$$

Unlike the case of pure hermaphroditism (2a), the rate of parent-sharing under androdioecy depends upon the uniparental proportion s_A .

We assign the arbitrary constant N in (8) as $(N_h + N_m)$, implying a scaled rate of coalescence of

$$C = \frac{(1 + s_A)^2}{4(1 - p_m)} + \frac{(1 - s_A)^2}{4p_m},$$

for

$$p_m = \frac{N_m}{N_h + N_m} \quad (\text{A.2})$$

the proportion of males among reproductive individuals.

A.3 Gynodioecy

Seed parents comprise N_f females and N_h hermaphrodites, with each female generating seeds at rate σ relative to each hermaphrodite. Females set all seeds from the population pollen cloud, which derives entirely from hermaphrodites. Hermaphrodites set a proportion a of their seeds by self-pollen and the remaining proportion from the population pollen cloud. Of biparental offspring (those derived from the pollen cloud), a proportion H (5) have a hermaphroditic seed parent and the complement a female seed parent.

Uniparental proportion: Ignoring terms of order $1/N_f$ or $1/N_h$, the uniparental proportion s^* corresponds to (4a):

$$s_G = \frac{\tau N_h a}{\tau N_h a + N_h(1 - a) + N_f \sigma},$$

for τ the rate of survival of uniparental offspring relative to biparental offspring.

Parent-sharing: A pair of uniparental individuals share their parent with probability $1/N_h$. A uniparental individual and a biparental individual share a parent with probability

$$H \frac{2}{N_h} + (1 - H) \frac{1}{N_h},$$

and two biparental individuals share exactly one parent with probability

$$H^2 \frac{4}{N_h} + 2H(1 - H) \frac{2}{N_h} + (1 - H)^2 \left[\frac{1}{N_f} + \frac{1}{N_h} \right], \quad (\text{A.3})$$

for H given by (5). In total, the probability that a pair of genes sampled from distinct individuals derive from the same parent ($1/N^*$) corresponds to (4b):

$$\begin{aligned} \frac{1}{N_G} &= s_G^2 \frac{1}{N_h} + s_G(1 - s_G)(1 + H) \frac{1}{N_h} + (1 - s_G)^2 \left[\frac{(1 + H)^2}{4N_h} + \frac{(1 - H)^2}{4N_f} \right] \\ &= \frac{[2 - (1 - s_G)(1 - H)]^2}{4N_h} + \frac{[(1 - s_G)(1 - H)]^2}{4N_f}. \end{aligned}$$

This expression depends on both the fraction of uniparental offspring (s_G) and the proportion of biparental offspring with a hermaphroditic seed parent (H).

We assign the arbitrary constant N in (8) as $(N_h + N_f)$, implying a scaled rate of coalescence of

$$C = \frac{[2 - (1 - s_G)(1 - H)]^2}{4(1 - p_f)} + \frac{[(1 - s_G)(1 - H)]^2}{4p_f},$$

for

$$p_f = \frac{N_f}{N_h + N_f} \tag{A.4}$$

the proportion of females (male-steriles) among reproductive individuals.

B Implementation of the MCMC

B.1 Efficient inference on selfing times through dynamic programming proposals

Simple Metropolis-Hastings (MH) proposals for T_k lead to extremely poor mixing efficiency. This is because the selfing time T_k and the coalescence indicators I_k are strongly correlated, so that changes to T_k will be rejected unless I_k is updated as well. For example, consider proposing a change of T_k from 1 to 0. When $T_k = 1$, on average half the I_{lk} will be 1 and half will be 0. $T_k = 0$ will always be rejected if any of the $I_{lk} = 1$, since the probability of a coalescence during selfing is 0 when there is no selfing. We therefore introduce a proposal for T_k that also changes I_k so that changes to T_k may be accepted.

The proposal starts from the value $T_k = t_k$ and proposes a new value t'_k . In standard MH within Gibbs, we would compute the probability of $T_k = t_k$ and of $T_k = t'_k$ given that all other parameters are unchanged. We modify this MH scheme to compute probabilities without conditioning on the coalescence indicators for individual k . However, the coalescence indicators for other individuals are still held constant. To compute this probability, let J indicate all the coalescence indicators I_y where $y \neq k$. Then

$$\Pr(\mathbf{X}, \mathbf{T}, \mathbf{J}, s, \theta) = \Pr(\mathbf{X}, \mathbf{J} | \mathbf{T}, s, \theta) \Pr(\mathbf{T} | s) \Pr(s) \Pr(\theta).$$

We introduce \mathbf{I}_k by summing over all possible values \mathbf{i}_k .

$$\Pr(\mathbf{X}, \mathbf{J} | \mathbf{T}, s, \theta) = \sum_{\mathbf{i}_k} \Pr(\mathbf{X}, \mathbf{I}_k = \mathbf{i}_k, \mathbf{J} | \mathbf{T}, s, \theta).$$

Since the i_{lk} for different loci are independent given T_k , we have

$$\begin{aligned} \Pr(\mathbf{X}, \mathbf{J} | \mathbf{T}, s, \theta) &= \sum_{\mathbf{i}_k} \prod_{l=1}^L \Pr(\mathbf{X}_l, I_{lk} = i_{lk}, \mathbf{J}_l | \mathbf{T}, s, \theta) \\ &= \prod_{l=1}^L \sum_{i_{lk}} \Pr(\mathbf{X}_l, \mathbf{I}_{lk} = i_{lk}, \mathbf{J}_l | \mathbf{T}, s, \theta). \end{aligned}$$

Therefore, for specific values of \mathbf{T} and \mathbf{J} , we can compute the sum over all possible values of \mathbf{I}_k for $l = 1 \dots L$ in computation time proportional to L instead of 2^L . This is possible because

the L coalescence indicators for individual k each affect different loci, and are conditionally independent given T_k and \mathbf{J} .

After accepting or rejecting the new value of T_k with I_k integrated out, we must choose new values for \mathbf{I}_k given the chosen value of T_k . Because of their conditional independence, we may separately sample each coalescence indicator I_{lk} for $l = 1 \dots L$ from its full conditional given the chosen value of T_k . This completes the collapsed MH proposal.

C Implementation of simulations

C.1 Simulated datasets

Our simulator (<https://github.com/skumagai/selfingsim>) was developed using `simuPOP`, publicly available at <http://simupop.sourceforge.net/>. It explicitly represents $N = 10,000$ individuals, each bearing two genes at each of L unlinked loci. Mutations arise at locus l at rate scaled rate θ_l (8), in accordance with the the infinite-alleles model.

We assigned values ranging from 0.01 to 0.99 to uniparental proportion s^* , with half of the $L = 32$ loci assigned scaled mutation rate $\theta = 0.5$ and the remaining loci $\theta = 1.5$. We generated simulated data under two sampling regimes: large ($L = 32$ loci in each of $n = 70$ diploid individuals) and small ($L = 6$ loci in each of $n = 10$ diploid individuals).

We conducted 10^2 independent simulations for each assignment of s^* . Each simulation was initialized with each of the $2N \times 32$ genes representing a unique allele. Most of this maximal heterozygosity was lost very rapidly, with allele number and allele frequency spectrum typically stabilizing well within $10N$ generations. After $20N$ generations, we recorded the realized population, from which 100 independent samples of $L = 32$ loci of size $n = 70$ were extracted. From this collection, we randomly chose $L = 6$ loci and subsampled 100 independent samples of of size $n = 6$.

To 10^2 independent samples from each of 10^2 independent simulations for each assignment of the uniparental proportion s^* , we applied our Bayesian method, the F_{IS} method, and RMES. Our Bayesian method is open-source and can be obtained at

<https://github.com/bredelings/BayesianEstimatorSelfing/>.

We used the implementation of RMES (David et al., 2007) provided at

<http://www.cefe.cnrs.fr/images/stories/DPTEEvolution/Genetique/fichiers%20Equipe/RMES%202009%282%29.zip>.

C.2 Indicators of accuracy

To compare the accuracy of our Bayesian method to RMES and the F_{IS} method, which produce point estimates, we summarize the posterior distribution of the uniparental proportion s^* by the median. Here, we compare the median to the mode and mean of the posterior distribution.

Figure 20 suggests that the bias and root-mean-squared (rms) error of these three indices exhibit different properties. For example, the posterior mode shows smaller bias throughout the parameter range, but the median and mean show smaller rms error for s^* near the boundaries (near 0 or 1).

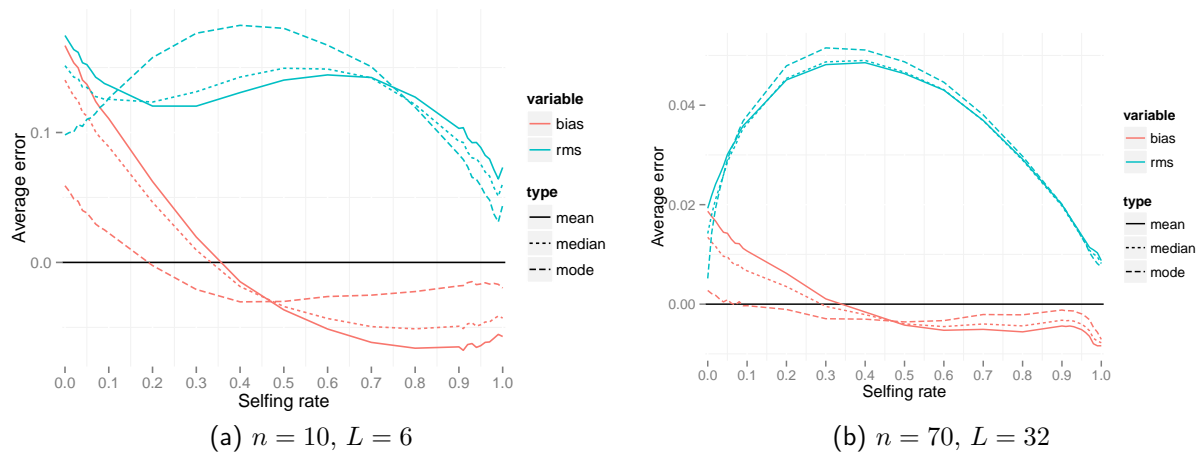


Fig. 20: Errors for the posterior mean, posterior median, and posterior mode. Blue curves (rms) indicate the root-mean-squared error, and red curves (bias) the average deviation. Averages are taken across simulated data sets at each true value of the selfing rate s^* .